Third AO4ELT Conference - Adaptive Optics for Extremely Large Telescopes
Florence, Italy. May 2013
ISBN: 978-88-908876-0-4
DOI: 10.12839/AO4ELT3.13344

A two deformable-mirror concept to improve the laser efficiency of Gemini South MCAO (GeMS)

Clémentine Béchet[1a], Andrés Guesalaga[1], Benoit Neichel[2], Vincent Fesquet[2], and Dani Guzman[1]

[1] Pontificia Universidad Catolica, Astro-Engineering Department, Santiago de Chile, Chile
[2] Gemini Observatory, La Serena, Chile

Abstract. GeMS is the first laser-based multi-conjugate adaptive optics (AO) offered to the astronomical community. Its asterism of 5 laser guide stars has recently proved to provide very uniform turbulence correction over the 85"x85" observation field, opening the new era of wide-field high angular resolution studies from the ground. Good AO performance requires however good wavefront sensing measurements from the laser guide stars, which directly depends on the quality of the laser spot images. The optimization of the lasers to be launched requires frequent calibrations and realignments to guarantee satisfying amplitude and phase of the projected beam. These complex and time-consuming procedures will strongly penalize the availability of GeMS. A laser beam shaping concept has been recently suggested to overcome such issues. It consists in applying, in the beam transfer optics, a field-conjugation thanks to 2 deformable mirrors (DM).
We remind this concept and discuss the criterion to be optimized and the desired amplitude and phase shapes at the output of the Gemini beam transfer optics. We investigate other amplitude shapes, as alternative from the classical gaussian beam, and we study in particular super-gaussian shapes of even orders. Two approaches are used : an analytical approximation of the criterion, and an estimation of it by numerical simulations of uplink laser propagation through the turbulence. Comparing the results obtained by the two approaches and analyzing their discrepancies, there seem to be no evident benefit to choose a super-gaussian beam shape of high order instead of a perfect gaussian amplitude from the point of view of the AO signal-to-noise ratio. As an additional result, the simulations highlight the potential assets of the 2-DM correction to avoid the aberrated amplitude actually measured on the laser and its associated degradation of the criterion by 30 to 50%.

1 The need for laser beam optimization

Good adaptive optics (AO) performance requires good wavefront sensing measurements from the guide stars because the AO correction quality is directly related to the measurement error [2]. For Shack-Hartmann (SH) wavefront sensors used in AO, the noise standard deviation σ_{meas} is, to the first order, proportional to the spot size and to the inverse of the square root of the number of photons received per subaperture and per frame, *i.e.* [3,4]

$$\sigma_{\text{meas}} \propto \frac{\sigma_{\text{image}}}{\sqrt{N_{\text{ph}}}}, \tag{1}$$

where σ_{image} is the standard deviation of the spot as seen in the focal plane of a SH subaperture, and N_{ph} is the average number of received photons per frame and per SH subaperture. The smaller the spot or the greater the number of received photons, the better the measurement accuracy. In particular, if the spot size is reduced by 30%, then the required number of photons for

[a] CBechetP@ing.puc.cl

a given measurement accuracy decreases by a factor 2. This is all the more important that for the 2 first years of operations of Gemini South multi-conjugate AO (GeMS) [1], in *low* Sodium season (December-January), the system is reported to often run at 200 Hz instead of 800 Hz in order to guarantee the detection of $\sim$ 135 photons / subaperture / frame allowing stable and good closed-loop AO correction [5]. As soon as a multi-laser AO system is designed with little margin in terms of expectable photon return, as is the case for GeMS, ensuring a small spot size σ is critical.

The spot size σ_{image} depends on various parameters, among which the laser spot intrinsic size, the potential elongation of the seen spot induced by the extension of the Sodium layer thickness in altitude, the SH subaperture size producing diffraction and the atmospheric seeing are of interest here. Typically, intrinsic laser spot size of full-width at half maximum (FWHM) 1.0 arcseconds are expected, and it has been actually observed on several laser systems like Gemini North Laser AO, Keck II LGSAO, and as well as on Gemini South GeMS [6].

In order to get the smallest intrinsic laser spot possible, the 589 nm beam needs to be diffraction-limited. In laser specifications, this translates into a single transverse mode $TEM_{0,0}$ and a beam quality factor $M^2 = 1$ at the Sodium layer [7]. Any discrepancy from this ideal shape results in M^2 values greater than 1. In the case of the Gemini South laser, diffraction-limited spot is currently not achievable. M^2 of 1.5 in x and 1.3 in y axis were measured during the length of the 2011/2012 commissioning campaign [6]. A slow increase of the M^2 values over each run has also been noticed, leading to conclude that the system gets misaligned with time. This degradation is understood as the result of quasi-static aberrations in both the laser bench and the Beam Transfer Optics (BTO) path.

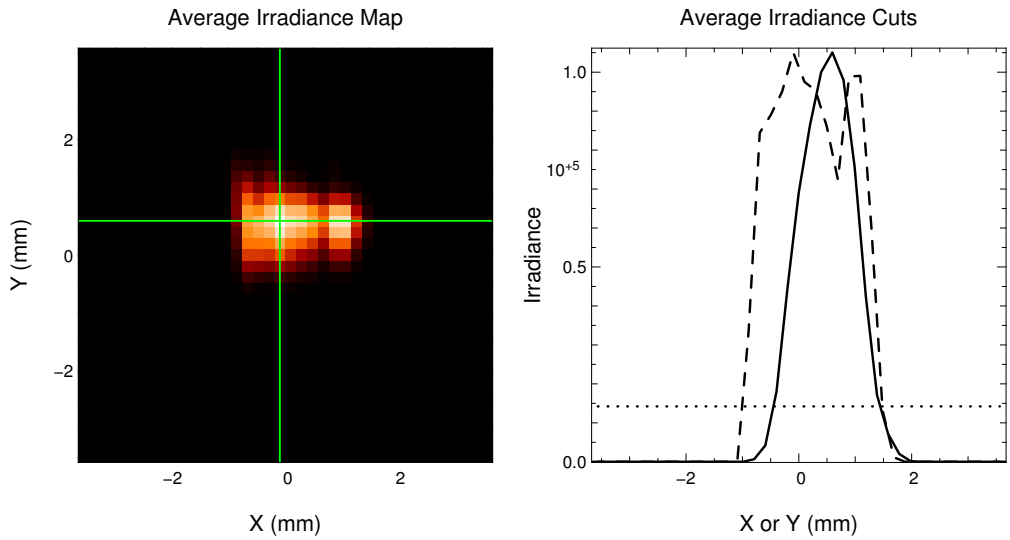

Fig. 1. Average irradiance map of the laser beam out of the laser bench during a run in April 2013. **Left :** Irradiance map. **Right :** Cuts along x (dashed) and y-axis (solid) of the irradiance map passing through the maximum (green lines on the left plot). The dotted horizontal line marks the $1/e^2$ limit.

In addition, Fig. 1 shows the results of measurements of the beam in April 2013, using a Shack-Hartmann sensor at the output of the laser bench. From these data, the M^2 factors have been estimated to be 2.22 and 1.21 along x and y directions respectively. The strong distortion in amplitude along x-axis is clearly visible in both plots of Fig. 1. The $1/e^2$ dotted line also shows that the diameter is 25% larger along x than along y. It is worth noting that the beam

quality is always worse in the x-axis because it corresponds to the unguided dimension of the Waveguide Amplifier Module amplification stages.

The optimization of the lasers launched out of the telescope requires to follow frequent and constraining calibrations and alignments procedures (quasi-static aberrations), in order to guarantee satisfying amplitude and phase of the beam. These complex and time-consuming procedures will strongly penalize the availability of GeMS [5,6]. In addition, the measurements presented in Fig. 1 were made after the alignment procedures, *i.e.* on the best laser shape at this time. It clearly appears that there is still need for an effort to improve the beam shape beyond this result. A controled beam shaping system described in the next section has been recently proposed to accelerate these optimizations of the laser.

2 The proposed 2-DM concept for beam shaping

A 2 deformable mirrors (DM) correction concept was proposed for GeMS [8] in order to compensate for distortions of its laser beam before the launch telescope. It is out of the scope of this paper to describe this system in details but we briefly remind its principle and its architecture in Fig. 2 (left). In order to ensure a diffraction-limited beam at the Sodium layer, correction for the quasi-static aberrations of both amplitude and phase is required. It is referred as optical field conjugation and it is realized thanks to 2 deformable mirrors (instead of just one when only phase compensation is enough). Optical field conjugation to correct for the atmospheric turbulence has generated a significant amount of interest during the last two decades in the fields of free-space telecommunications and weapon systems [9–12]. However, its application to astronomical purposes is new to our knowledge.

As can be seen on the left of Fig. 2, the collimated laser is supposed to fall upon DM1, where a phase shape is added to the wave. This applied phase aims at modifying the amplitude shape of the wave in the region of the second DM (at distance z). This second DM is optically conjugated to the pupil plane of the beam projecting aperture. The control of DM2 then only modifies the phase distribution of the output beam in the pupil plane of the projecting aperture. A sensing device is assumed to provide the necessary measurements to compute the control of the 2 DMs. Based on the desired beam shape at the projecting aperture, a phase retrieval method has been developed [8] to deduce the commands to be applied to the mirrors. It is an iterative algorithm using a weighted least-squares phase unwrapper.

The criterion driving the DMs control is built to reach a desired amplitude and phase shape on the projecting aperture. The choice of the desired amplitude shape is thus discussed in details in the following section.

3 Optimal beam amplitude shape?

Once the ideal 2-DM correction system exists, it is possible to obtain a desired amplitude and phase shape at the launch telescope. In design studies of laser launching systems, the projected wave is usually considered to have Gaussian amplitude (*e.g.* [13,14]) because the laser beam theoretically fits this shape. However, now that other amplitude shapes could be feasible with the 2-DM concept, new open questions arise :

- What is the optimal amplitude shape to be launched for the AO application?
- What about adapting the amplitude shape to the seeing conditions?

Both an analytical study in Sect. 3.1 and a modeling work linked to numerical simulations in Sect. 3.2 are developed here to provide a better understanding of the influence of the amplitude shape on the AO system error budget.

The chosen optimization criterion is the AO measurement noise level as approximated by Eq. (1), since minimizing this noise level is equivalent to minimizing the signal-to-noise ratio. This assumption is justified by the fact that the signal, *i.e.* the measured atmospheric turbulence, does not change with the beam shaping. From Eq. (1), the measurement noise level is directly related to the spot image size on the sensor and the received flux. These two quantities result from a process which can be decomposed in 2 main steps [14]: (i) the uplink propagation, from the launch telescope to the Sodium star in the mesosphere and (ii) the downlink propagation, from the Sodium star to the SH sensor.

The measurement noise thus verifies

$$\sigma^2_{\text{meas}} \propto \frac{\sigma^2_{\text{image}}}{N_{\text{ph}}} \propto \frac{\sigma^2_{\text{up}} + \sigma^2_{\text{down}}}{P_{\text{up}}} = \frac{\sigma^2_{\text{image}}}{P_{\text{up}}}\,, \tag{2}$$

where σ^2_{up} and σ^2_{down} characterize the uplink propagation and the downlink propagation contributions respectively. The former is the variance of the laser spot image in the Sodium layer, after uplink propagation. The latter is the variance of a point source imaged by the SH after downlink propagation. P_{up} is the energy projected up in the Sodium layer to form the laser spot, and we assume here that to a first order the number of returned photons increases linearly with this quantity. Dealing with a more accurate modeling of the Sodium return process is out of the scope of this study, however some recent works on the subject [15] could later be used to account for it in the simulations approach. The value of σ^2_{down} is driven by the wavefront sensor characteristics and the turbulence conditions, not by the beam shaping. Therefore, we focus our study on how the most right term of Eq. (2), our criterion, is influenced by the amplitude shape *via* σ^2_{up} and P_{up}.

Two class of amplitude shapes are considered, gaussian and super-gaussian (SG) of $p-$order. The radially symmetric complex amplitude u_p of the SG wave above the launching aperture follows the equation

$$u_p(r) = E_p\, \exp(-(r/w_0)^p)\,, \tag{3}$$

where r is the distance to the optical axis, w_0 is the beam $1/e^2$ radius at waist and E_p is a scalar normalization factor. For $p = 2$, Eq. (3) becomes the equation of a gaussian amplitude (SG of order 2). Figure 2 (right plot) illustrates the different radial shapes of gaussian (blue), SG of order 4 and SG of order 16 (black) amplitudes above the launching aperture including the truncation. The criterion $\sigma^2_{\text{image}}/P_{\text{up}}$ can now be optimized with respect to the order p and the truncation D/w_0, depending on turbulence conditions characterized by the Fried parameter r_0. Two different approaches are presented for this. The first approach, in Section 3.1, is based on analytical approximations. Next, Sect. 3.2 presents the results obtained by numerical simulations of uplink propagation.

3.1 from analytical approximations

The first approach was developed with the goal to derive an analytical expression of the criterion $\sigma^2_{\text{image}}/P_{\text{up}}$. Although gaussian wave propagation through random media have been

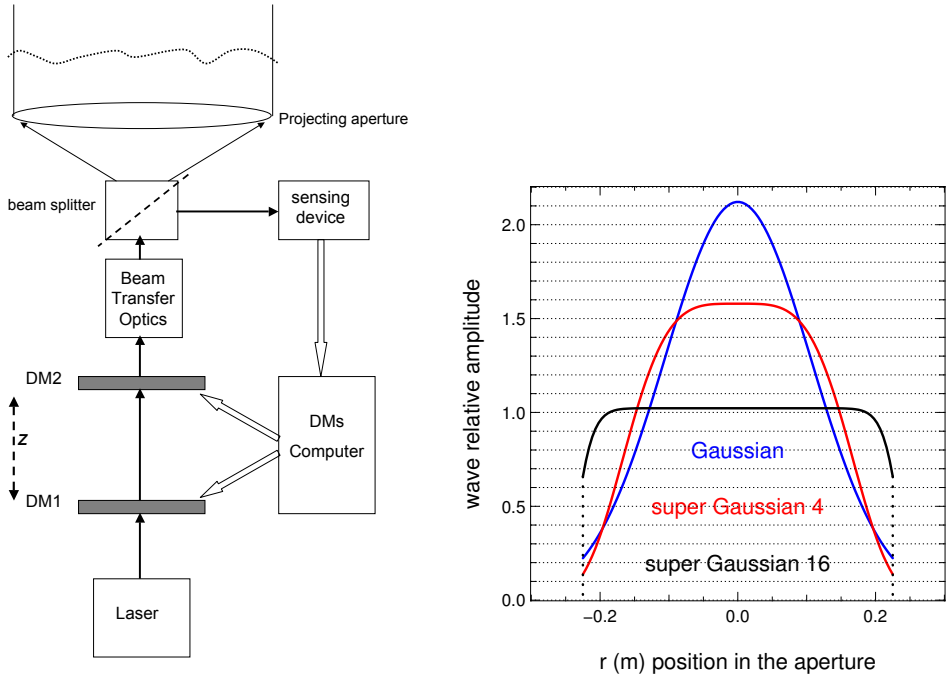

Fig. 2. Left : Architecture of the 2-DM correction of the laser before its projection. **Right :** Examples of beam amplitude shapes accross the launching circular aperture of 45 cm diameter. For all shapes, the amount of projected energy is equal to the amount projected by a uniformly illuminating plane wave of amplitude 1 among the aperture. Blue : gaussian shape. Red : SG of order 4. Black : SG of order 16. Dashed lines : limits of the projecting aperture.

extensively studied [7, 16, 17] for its wide range of applications in free-space laser communications and defense, the analytical formulae for other wave shapes are not available from the literature. Furthermore, the expression of the variance of the spot image $\sigma^2_{\rm up}$ involves an indefinite integral over the infinite field of view or a difficult evaluation through a convolution in case the field-of-view is truncated to define the integral for the variance properly. Therefore, to follow the analytical approach, we had to use the definition of an equivalent width $w_{\rm up}$ to characterize the spot size, instead of the variance of the image. Note that the approach developed here has been inspired from analytical studies of uniform plane wave [18] and gaussian wave [19] propagation through atmospheric turbulence.

Following the modeling of D. L. Fried [18] and extending it to radially symmetric amplitude shapes, the expression of the average short-exposure maximum irradiance $< I_{z\rm Na}(0) >$ at altitude $z_{\rm Na}$ in the Sodium layer leads to a triple integral which can be numerically evaluated. This maximum irradiance can thus be computed as a function of p the SG order, of D/w_0 the truncation and of D/r_0 the ratio between the aperture diameter and the Fried parameter, such that $< I_{z\rm Na}(0) >= f(p, D/w_0, D/r_0)$. The conservation of the energy finally leads to write

$$w^2_{\rm up} = \frac{4\,P_{\rm up}}{\pi < I_{z\rm Na}(0) >} \quad \text{and} \quad \frac{\sigma^2_{\rm image}}{P_{\rm up}} \simeq \frac{w^2_{\rm up}/(8\ln 2) + \sigma^2_{\rm down}}{P_{\rm up}}\,. \tag{4}$$

Figure 3 shows the criterion value obtained with 3 different shapes depending on D/w_0 and D/r_0 values. Only the cases of $D/r_0 = 3$ (left plot) and $D/r_0 = 4$ (right plot) are presented, being typical conditions with $r_0 = 15$ cm and $r_0 \simeq 11$ cm respectively at 590 nm at GeMS ($D = 45cm$).

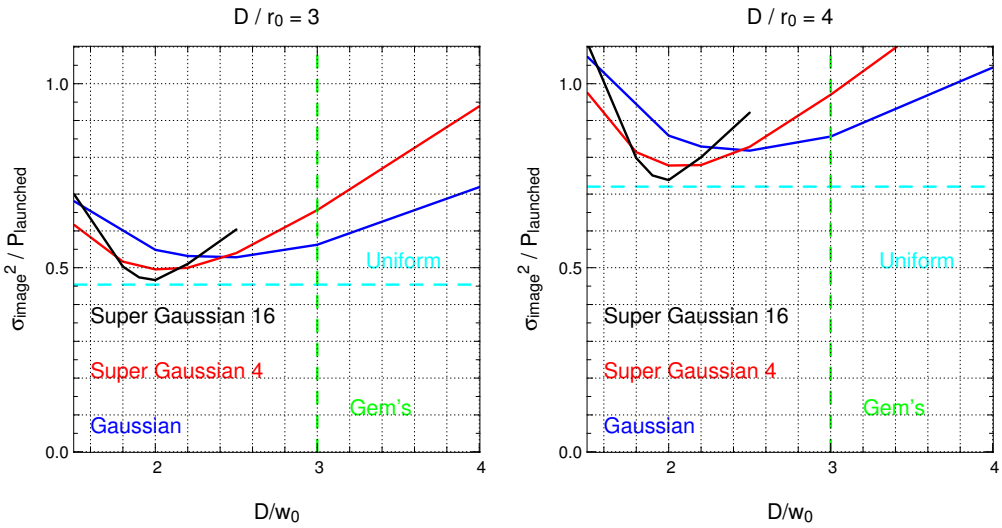

Fig. 3. Estimated values of criterion for various shapes, depending on D/w_0 and for typical r_0 values. $D/r_0(589\text{ nm}) = 3$ (left) and $D/r_0(589\text{ nm}) = 4$ (right). A launching aperture of $D = 45$ cm is considered as is the case in GeMS.

The results for the uniform and gaussian shapes are in agreement with the literature [18, 19], particularly showing increase of the optimal truncation D/w_0 when D/r_0 increases for gaussian. Note that in the range of D/r_0 between 3 and 4 in Fig. 3 this increase is hardly noticeable.

When SG of higher orders are used however, it clearly appears that the optimal truncation D/w_0 decreases with p. Higher orders also provide better (smaller) criterion optimal values, with about 15% reduced measurement noise in variance for SG of order 16 compared to gaussian. The criterion value is also more sensitive to D/w_0 (greater curvature) for higher SG orders. The green dashed line represents the D/w_0 fixed in GeMS, which has been designed for large D/r_0 (pessimistic conditions) assuming the laser would deliver a gaussian amplitude [13].

3.2 from numerical simulations of uplink propagation

Since the analytical approach followed in Sect. 3.1 uses approximations with an equivalent width to get the criterion estimate, we made a parallel study with simulations of the uplink propagation. The code consists in applying *angular spectrum propagation* steps to simulate Fresnel propagation from the launch telescope to the altitude zNa in the Sodium layer [14]. The spot size at this height, σ^2_{up} for Eq. (2), is estimated using the variance of the short-exposure image computed over the finite field-of-view of the GeMS SH subapertures. Although it would be possible to take into account the vertical distribution of the Sodium in altitude in the mesosphere [14], the presented results do not account for this. The criterion estimated values from the simulations with 50 randomly generated turbulent atmospheres are shown in Fig. 4.

Although the curvature around the optimum of the highest-order SG shapes is, like in Fig. 3, greater than for the gaussian shape, the best criterion is on the contrary here obtained for the gaussian. The criterion values are larger than in Fig. 3 for high-order SG. These poorer performance of SG, although closer to a uniform shape which theoretically provides the smallest FWHM, is understood to be due to the presence of higher frequencies. They spread more energy in the wings of the spot, which will be truncated by the limited field-of-view. These last results, which are not taken into account in the analytical approach, appear important in order

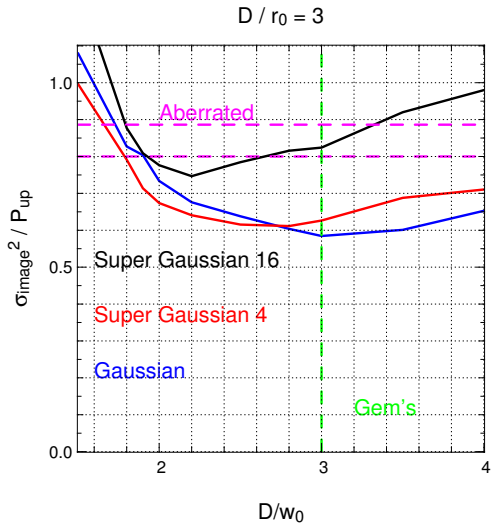

Fig. 4. Estimated values of criterion for various shapes using numerical simulations, depending on D/w_0 and for typical r_0 values such that $D/r_0(589\text{ nm}) = 3$. A launching aperture of $D = 45$ cm is considered as in the case of GeMS.

to highlight the risk of degradation from high frequencies in the amplitude. The smooth shape of the Gaussian seem crucial to effectively produce a small spot size.

Finally, it is possible to include in the simulations aberrations of amplitude at the launching aperture, in order to understand the potential effects of the beams distortions measured in Fig. 1. No phase aberrations were considered here. The degradation of the criterion value in such conditions is represented by the dashed pink lines in Fig. 4 (upper line for X-direction and lower line for Y-direction). The criterion value is degraded by 30% along $y-$axis and 50% along $x-$axis, compared to a perfect gaussian amplitude as specified in GeMS design (green dashed line for D/w_0). This last result highlights the potential benefit of the 2-DM correction which could deliver the desired gaussian amplitude at the launch telescope.

4 Conclusion

GeMS performance and availability is affected by complex and time-consuming realignment procedures of the laser for every new observation, and by the beam distortions actually observed out of the laser bench. This has led to the design of a 2-DM correction concept to apply optical field-conjugation on the laser path and thus produce an optimal amplitude and phase at the launching aperture. The determination of the desired amplitude shape for the beam is investigated with the aim to optimize a criterion directly related to the AO performance. The dependence of this criterion on the choice of the amplitude shape is studied, considering as alternative from a classical gaussian beam, super-gaussian shapes of even orders and variable sizes. Two approaches are compared to study such potential better shapes : an analytical approximation of the criterion, and an estimation of it by numerical simulations of uplink laser propagation through the turbulence.

The analytical approach predicts that a high-order super-gaussian (order-16) optimizes the criterion value by 15% compared to a gaussian. On the opposite, simulations of uplink propagation evaluating the criterion from the variance of the spot image over the WFS field of view, indicates that a super-gaussian shape increases the measurement error, compared to the classical

Gaussian. This enhances the drawback of super-Gaussian high frequencies, spreading energy at large distance from the axis. At the end of the day, there is no evident benefit for the AO performance to choose a super-gaussian beam shape of high order instead of a gaussian amplitude.

Finally, the simulations allow to study the effective impact of amplitude distortions as currently observed at GeMS. These distortions appear to decrease the signal-to-noise ratio of the AO system by 25 to 30%, compared to what a corrected gaussian amplitude could bring with the beam shaping procedure.

Aknowledgments

This work was supported by the Chilean Research Council (CONICYT) through grant Fondecyt 1120626.

References

1. F. Rigaut, B. Neichel, M. Boccas, C. d'Orgeville, G. Arriagada, V. Fesquet, *et al.*, *Proc. SPIE 8447, Adaptive Optics Systems III* **8447** (2012), pp. 8447OI.
2. F. Roddier, *Adaptive Optics in Astronomy*, (Cambridge U. Press, England, 1999).
3. G. Rousset, *Adaptive Optics in Astronomy* (F. Roddier, Cambridge U. Press, England, 1999), pp. 91–130.
4. S. Thomas, T. Fusco, A. Tokovinin, M. Nicolle, V. Michau, and G. Rousset, Mon. Not. R. Astron. Soc. **371**, (2006) pp. 323–336.
5. B. Neichel, F. Rigaut, A. Serio, G. Arriagada, M. Boccas, C. d'Orgeville, V. Fesquet, *et al.*, *Proc. SPIE 8447, Adaptive Optics Systems III* **8447** (2012), pp. 84470W–24.
6. C. d'Orgeville, S. Diggs, V. Fesquet, B. Neichel, W. Rambold, F. Rigaut, A. Serio, *et al.*, *Proc. SPIE 8447, Adaptive Optics Systems III* **8447** (2012), pp. 84471Q–21.
7. L. C. Andrews and R. L. Phillips, *Laser beam propagation through random media* (SPIE Optical Engineering Press, Bellingham, Washington USA, 1998).
8. A. Guesalaga, B. Neichel, M. Boccas, C. D'Orgeville, F. Rigaut, D. Guzman, and J. Anguita, *Proc. SPIE 8447, Adaptive Optics Systems III* **8447** (2012), pp. 84474M.
9. M. A. Vorontsov and V. Kolosov, J. Opt. Soc. Am. A **22** (2005), pp. 126–141.
10. Z. Zhao, S. D. Lyke, and M. C. Roggemann, *ICC'08* (2008), pp. 5432–5436.
11. M. C. Roggemann and D. J. Lee, Appl. Opt. **37** (1998), pp. 4577–4585.
12. R. Kizito, M. C. Roggemann, T. J. Schulz, and Y. Zhang, *Proc. SPIE 5160, Free-Space Laser Communication and Active Laser Illumination III* **5160** (2004), pp. 406–416.
13. C. D'Orgeville, B. J. Bauman, J. W. Catone, B. L. Ellerbroek, D. T. Gavel, and R. A. Buchroeder, *Proc. SPIE 4494, Adaptive Optics Systems and Technology II* **4494** (2002), pp. 302–316.
14. R. Holzlöhner, D. Bonaccini Calia, and W. Hackenberg, *Proc. SPIE 7015, Adaptive Optics Systems* **7015** (2008), pp. 701521.
15. R. Holzlöhner, S. M. Rochester, D. Bonaccini Calia, D. Budker, J. M. Higbie, and W. Hackenberg, A.&A. **510** (2010), pp. A20.
16. R. R. Parenti and R. J. Sasiela, *Tech. rep.*, (DTIC Document, 2005).
17. R. Fante, Proceedings of the IEEE **63** (1975), pp. 1669–1692.
18. D. L. Fried, J. Opt. Soc. Am. **56** (1966), pp. 1372.
19. H. T. Yura, Appl. Opt. **34** (1995), pp. 2774.